Available online at www.sciencedirect.com

ScienceDirect

Surface & Coatings Technology 201 (2007) 6667–6669

SURFACE & COATINGS TECHNOLOGY

www.elsevier.com/locate/surfcoat

Mechanical properties and Raman characterization of amorphous diamond films as a function of film thickness

Jiaqi Zhu *, Jiecai Han, Aiping Liu, Songhe Meng, Chunzhu Jiang

Center for Composite Materials, Harbin Institute of Technology, Post-box 3010, Yikuang Street 2, Nangang District, Harbin 150080, PR China

Abstract

Amorphous diamond (a-D) films with different thicknesses have been prepared on the c-Si substrate under the same deposition conditions using filtered cathodic vacuum arc (FCVA) technology. The film thickness was measured with a calibrated surface profiler. The mechanical properties were analyzed by a nano-indenter and the microstructure was characterized with visible Raman spectroscopy. It has been shown that the residual compressive stress of a-D films drops continuously down with increasing film thickness. When the films are thinner, the stress falls strikingly. However, the falling rate is less pronounced with the monotonic increase in film thickness. Hardness and Young's modulus also persistently rise with growing film thickness. Whereas the critical scratching load decreases at first and then increases again. The peak position of the asymmetric broad peak in the Raman spectra shifts towards low frequencies with increasing film thickness because of the monotonic fall in the residual compressive stress. However, the magnitude of the shift is smaller. Additionally, the Raman characterization is apt to be taken in the film thickness scope of 50–80 nm.

PACS: 78.30.Ly; 62.20.Qp

Keywords: Amorphous diamond; Filtered cathodic vacuum arc; Mechanical properties; Raman spectra

1. Introduction

Amorphous diamond (a-D) films have many beneficial properties like those of natural diamond due to its sp^3-rich bonds. Therefore, extensive applications can be found in different fields [1]. a-D films are generally deposited at room temperature with an energetic beam comprising pure carbon ions. The growth mechanism might be explained by the densification in the subplantation process [2]. Accordingly, high intrinsic stress consorting with the superexcellent properties restricts the maximal adhesive film thickness and inhibits popularization of a-D films. In addition, Raman spectroscopy is the best non-destructive way to obtain detailed bonding structure information. However, Raman measurements are sensitive to film thickness. In this work, the correlations between the mechanical properties, Raman spectra and the film thickness of a-D films are discussed.

2. Experimental

A series of samples with different film thickness were deposited on P(100) polished c-Si wafers at a negative bias of 80 V with the filtered cathodic vacuum arc (FCVA) system described in detail elsewhere [3]. Before deposition, the bare substrate was rinsed with acetone in a supersonic bath for 15 min and then was etched for 5 min by a Kaufman ion gun. The film thickness was measured with the calibrated KLA-Tencor P15 surface profiler and Dimension 3100 atomic force microscope after the marked lines were wiped off with acetone. Hardness, Young's modulus and scratching load were derived using an XP-Nanoindenter. The microstructure of the films was characterized with Renishaw RM1000 Raman spectrometer equipped with Ar^+ ion laser of 514.5 nm.

3. Results and discussion

3.1. The mechanical properties of the films

Fig. 1 shows that hardness and Young's modulus increase with the film thickness. As the film thickness surpasses 300 nm,

---

* Corresponding author. Tel./fax: +86 451 86407970.
E-mail address: zhujq@hit.edu.cn (J. Zhu).

0257-8972/$ - see front matter © 2006 Elsevier B.V. All rights reserved.
doi:10.1016/j.surfcoat.2006.09.062

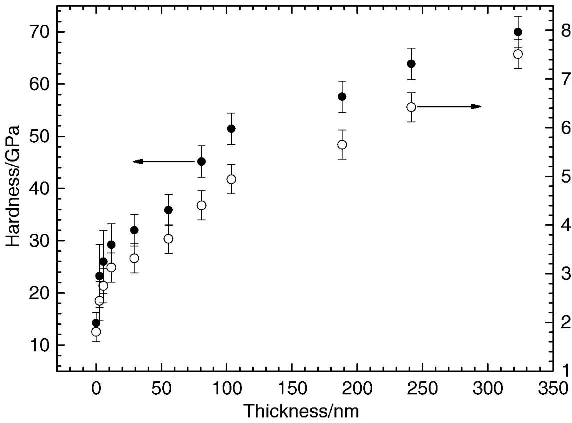

Fig. 1. Variations of hardness and Young's modulus as functions of film thickness. Every point represents the arithmetic mean of ten separate indents and the error bars are calculated from the standard deviation of the ten results.

hardness is close to 70 GPa and Young's modulus exceeds 750 GPa. In practice, the nanoindention hardness is determined from the load-unload curves using Pharr–Oliver methods [4]. This gives the mixed hardness of the silicon substrate and the a-D film. The thinner the film is, the more dramatic the influence of the substrate. Obviously, the real hardness and elastic modulus of the films are greater than the measured values. To remove the contribution of the "soft" substrate, the intrinsic hardness has been separated from the experimental substrate/film response by finite element modeling.

In Fig. 2, the critical scratching load falls strikingly with growing film thickness until about 100 nm. With the continuous increase of film thickness, a greater normal load is necessary to penetrate and scratch the films and the frictional force along the nick will rise again. Additionally, the critical scratching load is also determined by the required measurement inputs, compressive stress and the properties of the indenter and the film itself. Ref. [5] also believes that the thicker the film thickness is, the greater the critical scratching load. But Ref. [6] has induced an ultimately contradictory result. The reasons are not clear at present.

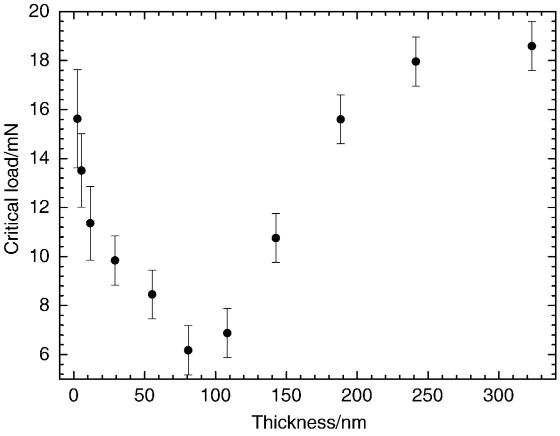

Fig. 2. Critical scratching load versus the film thickness. Each point represents the average of five separate scratches, and the error bars are deduced from the standard deviation of these five results.

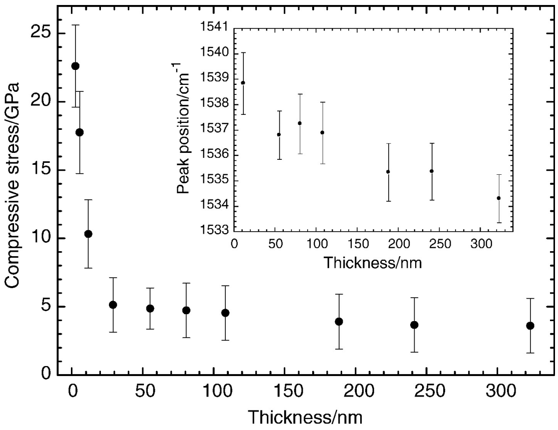

Fig. 3. Variation of compressive stress as a function of film thickness. The inset shows the position of the asymmetric Raman broad peak versus film thickness.

3.2. Stress and Raman measurements

According to Stoney's equation, the compressive stress was evaluated by comparing the curvature of the silicon substrate coated with the film against the curvature of the bare silicon substrate. It has been shown in Fig. 3 that the stress of the film continuously decreases with the increase of the film thickness. When the film is thinner, the descending trend becomes greater because the interfacial tension becomes more remarkable. And then, the stress drops mildly because partial relaxation of internal stress takes place owing to the accumulation of the surplus energy during deposition. The compressive stress is lower because of the application of a high pulse bias.

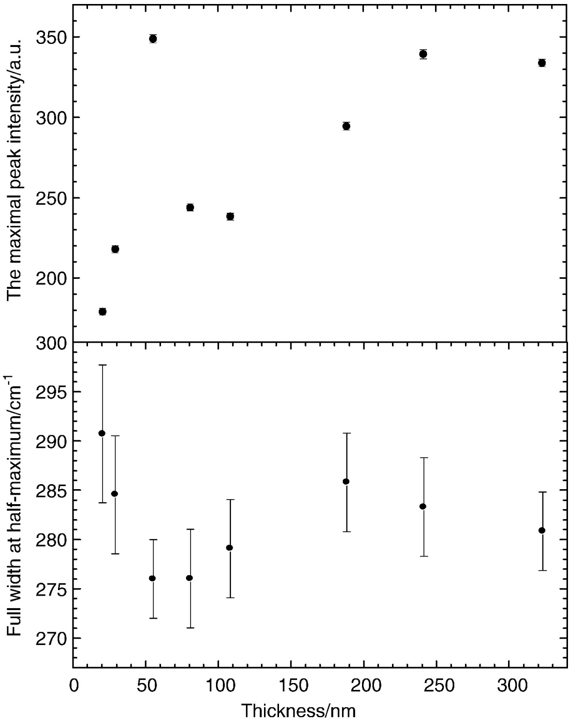

Fig. 4. The maximal peak intensity and full-width at half-maximum as functions of film thickness.

The inset in Fig. 3 illustrates that the position of the asymmetric Raman broad peak fitted by Breit–Wigner–Fano lineshape shifts towards low wavenumber values with increasing film thickness. It has been observed that stress can shift the Raman scattering feature to the higher frequencies by 20 cm^{-1} before and after the films delaminate from the substrate [7]. If the asymmetric broad peak is deconvoluted into two peaks, the G-peak of the Raman spectrum can shift more significantly to higher wavenumbers by 4.1 ± 0.5 cm^{-1}/GPa due to the large residual compressive stress [8]. Since the stress falls with growing film thickness, it can be seen that the Raman peak position moves towards low frequencies with increasing film thickness. Additionally, the cross-sectional structure of a-D films is generally observed as a “sandwich” planar distribution [9]. The surface layer generated during the subimplantation process of film growth consists of sp^2-rich carbon domains and quasicontinuous two-dimensional structure in the manner of entangled ribbons, rings or chains [2]. The interlayer under the surface layer is rich in sp^3 components. The thinner the films are, the higher the proportion and influence of the sp^2-rich surface layer [10]. According to the three-stage model for the Raman interpretation [11], the G-peak position should shift toward high wavenumbers if the film thickness increases. However, the falling stress influences the Raman shift more intensively than the change of hybridization cross-sectional structure with film thickness.

Fig. 4 shows that the maximal intensity of the broad peak is the largest and the full width at half-maximum (FWHM) is the smallest when the film thickness is in the range of 50–80 nm. These results indicate that the Raman spectra are most prominent and convenient to investigate in the film thickness range. In addition, there seems to be a periodic trend of variation in the maximum peak intensity and its full width at half-maximum versus increasing film thickness because of the laser interference in the films.

4. Conclusion

Hardness and Young’s modulus of a-D films persistently rise with growing film thickness. Whereas the critical scratching load descends at first and then ascends again with increasing film thickness. The residual compressive stress of the films falls continuously with increasing film thickness. When film is thin, the stress falls strikingly. However, the falling tendency reduces with the monotonic increase of film thickness. The position of the asymmetric Raman broad peak shifts towards low frequencies with increasing film thickness because of the continuous decrease of the residual compressive stress. However, the magnitude of the shift is smaller owing to the cross-sectional “sandwich” microstructure of the films. Additionally, the Raman characterization of the films is apt to be taken in the range of film thickness 50–80 nm because the peak intensity is the largest and the full width at half-maximum is the smallest in this range.

Acknowledgement

This work was partially supported by the Development Program for Outstanding Young Teachers in Harbin Institute of Technology (HIT 2006). The authors would like to thank Ms. Tao Yanchun in Jilin University for Raman measurements.

References

[1] J. Robertson, Mater. Sci. Eng., R Rep. 37 (2002) 129.
[2] Y. Lifshitz, S.R. Kasi, J.W. Rabalais, W. Eckstein, Phys. Rev., B 41 (1990) 10468.
[3] J. Zhu, J. Han, S. Meng, J. Wang, W. Zheng, Vacuum 72 (3) (2003) 285.
[4] W.C. Oliver, G.M. Pharr, J. Mater. Res. 7 (1992) 1564.
[5] J. Qi, C.Y. Chan, I. Bello, C.S. Lee, S.T. Lee, J.B. Luo, S.Z. Wen, Surf. Coat. Technol. 145 (2001) 38.
[6] D. Sheeja, B.K. Tay, S.P. Lau, K.W. Leong, C.H. Lee, Int. J. Mod. Phys. B 16 (6–7) (2002) 958.
[7] J.W. Ager III, S. Anders, A. Anders, I.G. Brown, Appl. Phys. Lett. 66 (1995) 3444.
[8] J.K. Shin, C.S. Lee, K.R. Lee, K.Y. Eun, Appl. Phys. Lett. 78 (2001) 631.
[9] C.A. Davis, G.A.J. Amaratunga, K.M. Knowles, Phys. Rev. Lett. 80 (1998) 3280.
[10] S. Waidmann, M. Knupfer, J. Fink, B. Kleinsorge, J. Robertson, Diamond Relat. Mater. 9 (2000) 722.
[11] A.C. Ferrari, J. Robertson, Phys. Rev., B 61 (2000) 14095.